Article

Influence of Multiple Interactions of Three Typhoons and a Mid-Latitude Cloud Band-Associated Trough in the North West Pacific upon Severe Tropical Storm Linfa

Soo-Min Choi [1] and Hyo Choi [2],*

[1] Department of Computer Engineering, Konkuk University, 268 Chungwon-daero, Chungju 27478, Republic of Korea; fuledoc@hanmail.net
[2] Atmospheric & Oceanic Disaster Research Institute, Dalim Apt. 209 ho, Songjungdong 940-23, Gangneung 25563, Republic of Korea
* Correspondence: du8392@hanmail.net; Tel.: +82-10-7240-0357

Abstract: Multiple interactions of three typhoons and a mid-latitude cloud band-associated with a trough (MLCT) were investigated from 1 July to 10 July 2015, using the Korea Communication, Ocean, and Meteorological Satellite (COMS) satellite images and two kinds of meteorological models, such as UM-KMA (U.K.) and WRF-3.6 (U.S.A.), to generate the horizontal structure of wind and relative humidity, streamline, and moisture flux. As severe tropical storm (STS) Linfa moved toward the warmer area with a sea surface temperature (SST) of 31 °C in the northern South China Sea, it obtained not only more moisture by thermal convection of water vapor from the sea surface toward the lower atmosphere but also more momentum by its multiple interactions with both the MLCT and Typhoon (TY) Chan-Hom. Through their mutual interactions, mutual feedback of moisture and momentum fluxes could accelerate the formation of clouds in their systems and an asymmetric structure of their circulations. After Linfa weakened due to the increased friction of the shallower sea bottom close to the Chinese coast and its disconnection from the MLCT, later it became re-intensified with the increased wind speeds by a stronger interaction with more intensified TY Chan-Hom entering the path of the Kuroshio Current of SST 31 °C, which could supply additional moisture through thermal convection of water vapor into its system. Then, further interaction between the rapidly developed TY Nangka following behind and the MLCT enhanced the transfer of moisture and momentum fluxes from Chan-Hom into Linfa. Finally, after STS Linfa made landfall on the Chinese coast, it decayed into a weak low-pressure system before its dissipating, due to the weakening of its cyclonic circulation through the increased friction by the shallower sea bottom and the surrounding lands.

Keywords: multi-interaction of three typhoons; MLCT; sea surface temperature; moisture and momentum fluxes; thermal convection; Kuroshio current

1. Introduction

In recent years, tropical cyclones (called typhoons in Asia) have caused very high damage costs and severe casualties on and adjacent to their paths in East Asia. Anthes and Chang [1] and Choi [2] explain that typhoons always accompany heavy precipitation, producing floods, extremely strong winds, storm surges, and large ocean waves causing coastal erosion, the destruction of roads, farm fields, and houses, and damage to shipping. Hong Kong Meteorological Observatory [3] classifies tropical cyclones into six classes of typhoon: Super Typhoon, Severe Typhoon, Typhoon, Severe Tropical Storm, Tropical Storm, and Tropical Depression. These classes are based on 10-minute sustained wind speed thresholds around the typhoon center, as recommended by the World Meteorological Organization [4]. The Korean Meteorological Administration [5] defines the classification of tropical cyclones into four categories: Typhoon, Severe Tropical Storm, Tropical Storm,

and Tropical Depression, depending on the surface atmospheric pressure and wind speed near the typhoon center.

It is known that typhoons affect the marine and atmospheric environment through complex interactions. Choi [6] explained that an extreme cold sea outbreak near Cheju Island, Korea, took place under the influence of strong wind and atmospheric pressure change from typhoon Rusa. In another study by Choi et al. [7], the occurrence of cold sea surface temperatures (SSTs) near Cheju Island was produced from the response to strong cyclonic winds and a positive geopotential tendency following the track of a typhoon center. Subrahmanyam [8] also investigated the impact of a typhoon on the northwest Pacific sea surface temperature, while Latif et al. [9] described the effect of tropical sea surface temperature and vertical wind shear on the development of a hurricane.

Feng and Subrahmanyam [10] explained the chlorophyll variations across the coastal area of China from the effects of typhoon Rananim. Price [11] and Gill [12] described a model to explain the upper ocean response to a hurricane, while Knauss [13] suggested relatively simple methods to explain the response. Franklin, et al. [14] used nested analyses of dropwindsonde and Doppler radar data to explain the kinematic structure of Hurricane Gloria. Sheng et al. [15] also used a nested-grid ocean model in a numerical study to investigate a storm-induced circulation on the Scotian Shelf during Hurricane Juan, while Cheung and Chan [16] carried out improvements in wind and rain simulations for tropical cyclones with the assimilation of Doppler radar data. Dhana and Annapurnaiah [17] used the WRF-3.6 model to determine the best microphysics schemes for accurate simulation of a tropical cyclone's track and intensity. Shyam and Sharma [18] suggested an evaluation method on the accuracy of modeling ocean surface winds generated by tropical cyclones.

Fujiwhara [19] explained that when two cyclones are close enough to each other, they tend to rotate cyclonically about each other, moving around a common central pivot point and acting like a centroid. Liu [20] also showed the detailed relative motion of typhoon pairs over the South China Sea and Northwest Pacific Region. DeMaria and Chan [21] gave comments on a numerical study of the interactions between two cyclones, and Kuo et al. [22] explained the merger of the tropical cyclones "Zeb and Alex". Xu et al. [23] described the impact of tropical storm Bopha on the intensity change in the super typhoon in the 2006 typhoon season. Choi and Lee [24] showed that tropical storm Sarika was found to merge with the circulation of typhoon Songda by interacting with its strong wind field and moisture transport. Yeh et al. [25] explained that, interestingly, the intensification and decay of typhoon Nuri occurred through the influence of a cold front and south-westerly wind; this was explained with the aid of satellite cloud images.

However, as far as the authors are aware, there has been no detailed explanation of complex interactions associated with three typhoons and a mid-latitude cloud band-associated trough (MLCT). It is known that the North Pacific High is a semi-permanent subtropical anti-cyclone with a clockwise circular on the eastern side of Japan; the north-eastern Pacific Ocean; northeast of Hawaii; west of California; and part of the great belt of anticyclones at the subtropical ridge. It is strongest during the northern hemisphere summer and shifts towards the equator during the winter, when the Aleutian Low becomes more active (Wikipedia [26] (https://en.wikipedia.org/wiki/North_Pacific_High, accessed on 10 January 2023)).

Namely, the MLCT called a mid-latitude cloud band-associated trough is located between a low pressure in the north and a mid-latitude high pressure (or the North Pacific Ocean High Pressure with a clockwise circulation (NPOHP) between the latitudes of 20°N and 40°N. A large amount of moisture flowing along the MLCT produced a large cloud band oriented from southwest to northeast. Thus, the northwesterly (southwesterly) wind blows in the north (south) of the MLCT with a lot of moisture to form cloud clusters, resulting in heavy precipitation.

The purpose of this study is to investigate how the interacting processes with the MLCT formed along the northern edge of the North Pacific High Pressure, drawing a clockwise motion of air, typhoon (TY) Chan-Hom and TY Nangka, and also elevated SST

associated with the Kuroshio warm current of 31 °C, which could have influenced the reinforcement and decay of severe tropical storm (STS) Linfa in the South China Sea. We try to explain in detail, using satellite images, synoptic charts, and numerical simulation results of vertical and horizontal structures of the wind, and relative humidity, streamline analysis, and moisture flux.

2. Study Area and Numerical Model Experiments

2.1. Geography of the Study Area

The study area in East Asia includes the South China Sea, the East China Sea, the Yellow Sea, the Sea of Japan/the East Sea, and the Western Pacific Ocean facing Vietnam, China, the Philippines, Korea, Japan, and Russia in Figure 1. More than thirty tropical cyclones passed by those seas from the early summer to the late fall and caused severe weather with heavy rainfall and strong gusts in southern and northeastern Asia. In those seas, tropical cyclones have normal or abnormal tracks in their routes, and mutual interactions between two or three typhoons and a mid-latitude high pressure occur frequently.

Figure 1. Geography of East Asia.

2.2. Numerical Method and Input Data

Streamline analyses showing isotachs as lines of equal wind speed greater than 25 kt (≈12.5 m/s) and moisture flux, directly reflecting the flow of moisture corresponding to the wind direction and speed, were calculated using a version of the British Unified Model (UM) adopted by the Korean Meteorological Administration (KMA), called the UM-KMA model. The UM model consists of a numerical weather prediction and climate modeling software suite based on grid points rather than a spectral representation of the atmosphere and was originally developed by the United Kingdom Meteorological Office. Thereafter, this model has been further modified for local and regional scale forecasting by the KMA [5].

The original UM model consists of a software suite written in Fortran-90 and it uses initial input data provided by observations from satellites, ground-based weather stations, marine buoys, data from radar, radiosonde weather balloons, wind profilers, commercial aircraft, and a background meteorological field derived from preceding model runs [24]. The UM-KMA model uses nesting techniques for horizontal grid domains of 1.5 km and 4 km for representing areas such as the size of a city, 12 km for regional-scale domains, and 40 km for a global-scale domain. The streamline analyses and moisture flux fields were evaluated to investigate how a typhoon can intensify using the supply of moisture and momentum transfer into its system through complex interactions between the three typhoons and a cloud-associated mid-latitude trough.

Additionally, we also used a three-dimensional Weather Research and Forecasting Model (WRF)-3.6, which was adopted for a 96 h numerical simulation on meteorological elements such as wind, temperature, potential temperature, potential vorticity, etc., in northeast Asia. In the numerical simulation, one way, triple nesting process from the first domain to the third domain was performed with horizontal grid spaces of 27 km, and 3 km covering a 91×91 grid number in each domain, respectively, in the figures. National Centers for Environmental Prediction/National Center for Atmospheric Research (NCEP/NCAR) reanalysis–final analyses (FNL) $1.0° \times 1.0°$ resolution data were used as meteorological input data to the model and vertically interpolated onto 36 levels with sequentially larger intervals increasing with a height from the surface to the upper boundary level of 100 hPa.

In the model, WSM 6 scheme was used for heat and moist budgets and microphysical processes in the atmospheric boundary layer, and the YSU PBL scheme was adopted for the planetary boundary layer. The Kain–Fritsch scheme (new Eta) was adopted for cumulus parameterization and the fifth thermal diffusion model was employed for land surfaces. Simultaneously, the RRTM long-wave radiation scheme and dudhia short-wave radiation schemes were also used.

2.3. Satellite Data

The Communication, Ocean, and Meteorological Satellite (COMS) mission, in other ways known as 'Cheollian-1' or 'GEO-Kompsat-1', was launched in June 2010 and was primarily operated by the Korean Meteorological Administration (KMA). KARI (Korean Aerospace Research Institute), and KIOST (Korean Institute of Ocean Science and Technology) also assisted in the operation of COMS whilst it worked to monitor meteorological phenomena (cloud, wind, temperature, etc.) and ocean ecosystem phenomena (sea surface temperature, salinity, chlorophyll-a, wind waves, current speed, etc.), pollution (dust, etc.) as well as experiments with communication technology.

In this study, every one-hour, COMS satellite images were used to find the cloud area and the interaction of typhoons compared to weather maps. More precise analysis of COMS images is explained sequentially.

3. Results

In July 2015, several tropical cyclones were detected every few days in the west Pacific Ocean. The Joint Typhoon Warning Center (JTWC) monitored a small tropical disturbance in the Inter-tropical Convergence Zone (ITCZ) on 25 June and issued a Tropical Cyclone Formation Alert for a low pressure located about 350 km northeast of Pohnpei Island, Micronesia, at 22:30 Universal Time Coordinated (UTC; for instance, 09:00 Korean Local Standard Time (09:00 LST) = 09 h + 00:00 UTC), on 29 June 2015 [26]. The JTWC and the Japan Meteorological Agency (JMA) upgraded this system to a tropical depression (TD) at 00:00 UTC, on 30 June. It was then upgraded to a tropical storm (TS) by JMA, later assigned the name, Chan-Hom (No. 1509), and upgraded again to a typhoon (TY) on 1 July (Figure 2).
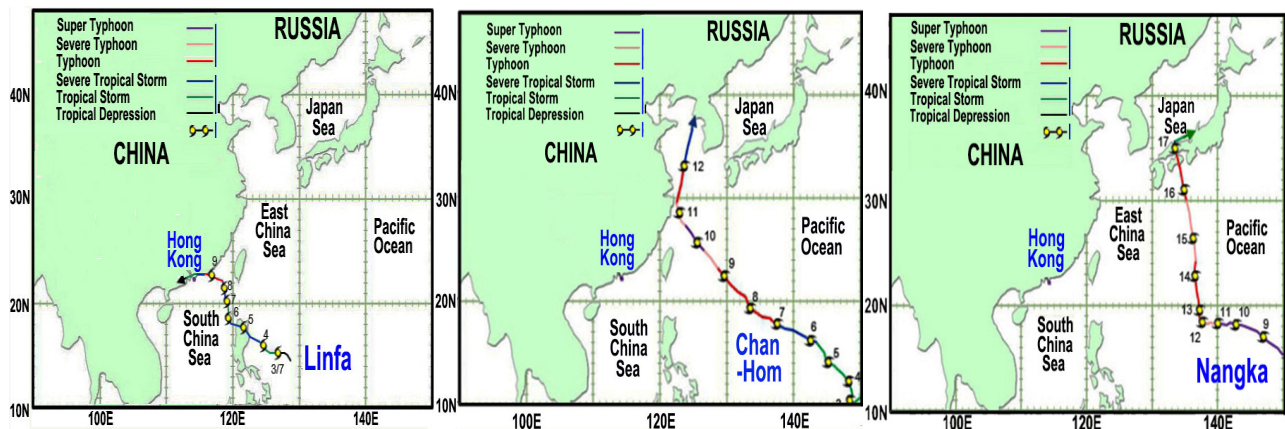
Figure 2. Typhoon tracks—STS Linfa, TY Chan-Hom, and TY Nagka (supplied by Hong Kong Observatory). Numbers (1 to 14) inside figures denote the day of July (https://www.hko.gov.hk/en/wxinfo/currwx/tc_gis.htm, assessed on 7 April 2015).

On the following day, the JTWC detected a tropical depression (TD) moving north-northwest, which formed over the Pacific Ocean east of the Philippines at 08:00 UTC, on 2 July. The tropical depression intensified into a tropical storm (TS) 12 h later and was named Linfa (No. 1510). Then, at 20:00 UTC, 4 July, Linfa further intensified into a severe tropical storm (STS) with a maximum surface wind of 24 m/s (Table 1).

Table 1. Comparison of TY-1509 Chan-Hom (C), STS-1510 Linfa (L), and TY-1511 Nangka (N) from 4 to 10 July 2015. "(+)" and "(−)" indicate the increase and decrease in surface pressure, and maximum surface wind speed for 24 h, respectively (data were supplied by the KMA).

Date	Surface Pressure (hPa)	Position	Maximum Surface Wind (m/s) (kt)	Moving Speed (km/h)
TS-L 09:00 LST, 4 July	990	15.3°N; 124.2°E	24 (48)	3
TY-C	985	12.4°N; 148.2°E	27 (54)	21
TY-N	1000 (a low)	10.2°N; 170.0°E	18 (36)	25
STS-L 09:00 LST, 5 July	985 (−5)	17.2°N; 122.1°E	27 (54) (+3)	11
TY-C	985 (0)	14.2°N; 144.8°E	27 (54) (0)	11
TY-N	990 (−10)	11.5°N; 164.8°E	24 (48) (+6)	20
STS-L 09:00 LST, 6 July	992 (+7)	18.5°N; 119.4°E	23 (46) (−4)	11
TY-C	980 (−5)	16.3°N; 142.5°E	29 (58) (+2)	19
TY-N	980 (−10)	11.7°N; 159.9°E	29 (58) (+5)	29
STS-L 09:00 LST, 7 July	985 (−7)	20.2°N; 119.0°E	27 (54) (+4)	4
TY-C	975 (−5)	18.0°N; 137.6°E	32 (64) (+3)	21
TY-N	950 (−30)	13.1°N; 155.5°E	43 (86) (+14)	25
STS-L 09:00 LST, 8 July	985 (0)	21.6°N; 118.7°E	27 (54) (0)	11
TY-C	960 (−15)	19.4°N; 133.4°E	39 (78) (+7)	17
TY-N	925 (−25)	15.6°N; 151.1°E	51 (102) (+8)	24
STS-L 09:00 LST, 9 July	980 (−5)	22.5°N; 117.7°E	29 (58) (+2)	13
TY-C	955 (−5)	22.5°N; 129.5°E	40 (80) (+1)	23
TY-N	935 (−10)	17.0°N; 146.9°E	49 (98) (−2)	20
STS-L 09:00 LST, 10 July	1000 (a low)	22.6°N; 112.4°E	Unreported	23
TY-C	935 (−20)	25.7°N; 125.6°E	49 (98) (+9)	20
TY-N	920 (−15)	18.2°N; 142.7°E	53 (106) (+4)	16

Based on the surface pressure chart, the COMS-IR image and models analyzed moisture flux and streamline analysis at 850 hPa level (approximately at 1.5 km height) and indicated the existence of STS Linfa and TY Chan-Hom at 00:00 UTC, 4 July, in our model domain. The two typhoons appear weakly connected via moisture flux (Figures 3 and 4a),

in comparison to clearly no connection to each other on 3 July. Nevertheless, any interaction between the two in terms of streamline analysis is negligible (Figure 4b).

(a)　　　　　　　　　　　　　　　　　(b)
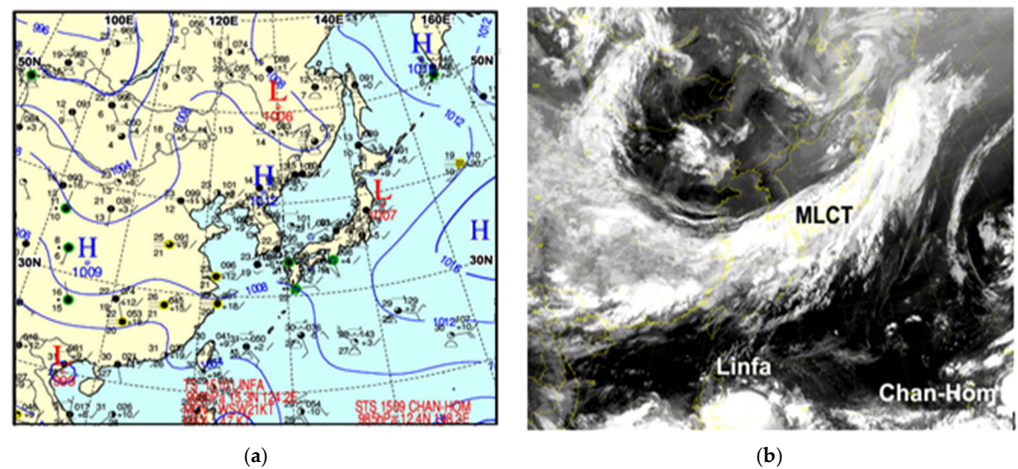
Figure 3. (**a**) Surface pressure chart and (**b**) COMS-IR satellite image at 09:00 LST, 4 July 2015. Small black circles of observation points in (**a**) denote clouds and precipitation. The MLCT indicates a mid-latitude cloud band-associated trough between a low pressure in the north and the North Pacific Ocean High Pressure (H on the right edge of (**a**)) between the latitudes of 20°N and 40°N.

(a)　　　　　　　　　　　　　　　　　(b)
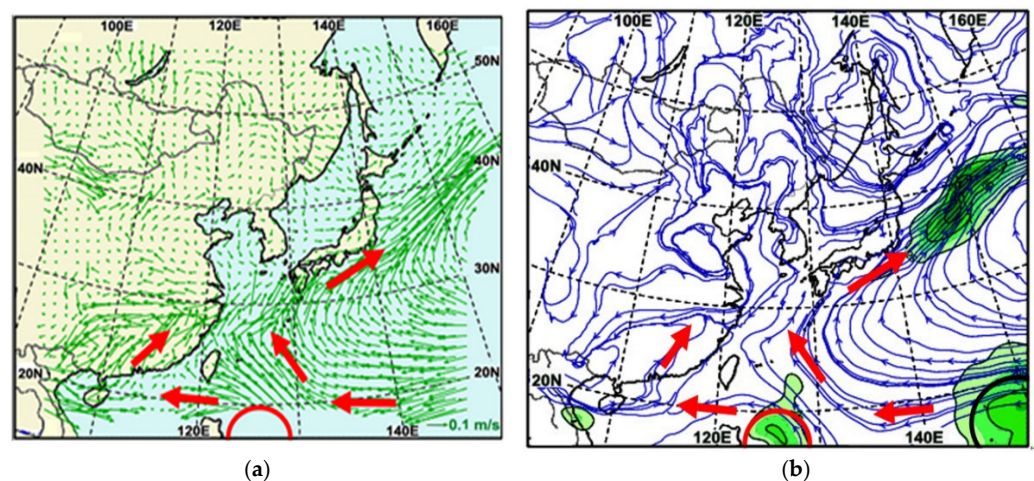
Figure 4. (**a**) Moisture flux (0.1 kg·m/s) and (**b**) streamline with isotachs (green color areas greater than 25 kt) at 850 hPa (1.5 km height) at 09:00 LST, 4 July 2015. TS Linfa (bottom-center) moving west-northwestward and TY Chan-Hom (bottom-right) moving westward were steered northwards by the southwest wind ahead of the MLCT enabling their cyclonic circulations to intensify when no interaction between tropical cyclones existed. Moisture converged into the MLCT.

Even though COMS-IR images showed the two tropical cyclones close to one another, their circulations were independent. However, they both interacted with a cloud band-associated mid-latitude trough extending from southern China to the northeast of Japan (Figure 5a). As shown in the figures, a large amount of moisture flows along the north edge of the NPOHP (H in the middle of the right side of Figures 3a and 5a), which is called the mid-latitude high pressure in another way, with its clockwise circulation of air. This moisture forms the MLCT between a low-pressure at high latitude and the MLHP, in structure by a north-westerly (south-westerly) wind regime in the north (south) of the MLCT.

(a)   (b)
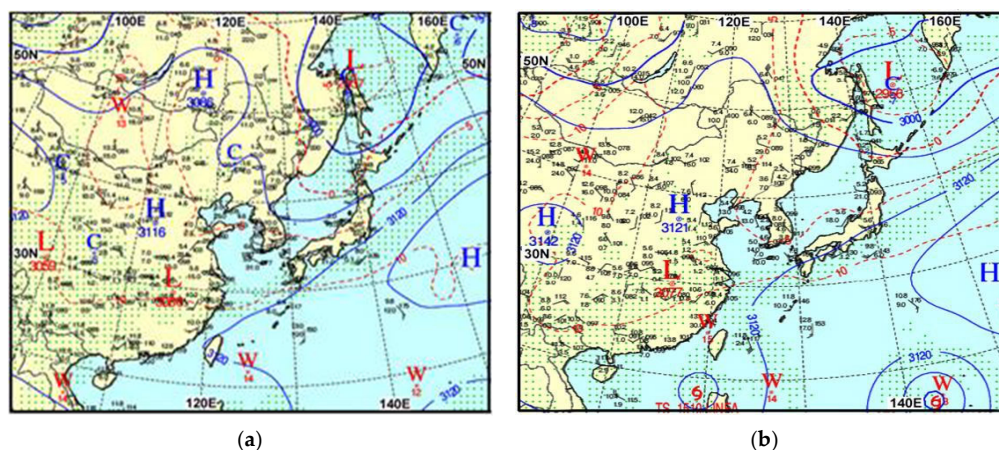
Figure 5. (**a**) Geopotential analysis (m) at 700 hPa (approximately 3 km height) at 09:00 LST, 4 July 2015, and (**b**) 09:00 LST, 6 July 2015. The distribution of small green-colored dots (clouds) oriented southwest to northeast through southern China indicate the MLCT located between a low pressure in the north and the North Pacific Ocean High Pressure (H) on the right in (**a**) and (**b**). Thus, clouds cover from 1.5 to 3 km in height.

From 4 July through 5 July, STS Linfa moved toward Taiwan Island and TY Chan-Hom moved toward the southern coast of Rota in the Mariana Islands. STS Linfa and TY Chan-Hom moved west-northwestward independently before they were steered northwestward by the northeastward movement in the MLCT. The interaction of the MLTTC with both STS Linfa and TY Chan-Hom strengthened Linfa's cyclonic circulation in its right upper quadrant to a maximum wind speed of 27 m/s with an increase of 3 m/s and a central pressure of 985 hPa with a decrease of 5 hPa in STS Linfa.

However, there was no change in central pressure or maximum surface wind speed of TY Chan-Hom, as indicated by the surface pressure chart, satellite image, and both moisture flux and streamline analyses charts at 850 hPa, and geopotential height at 700 hPa (Figures 3–5). Although the northeastward movement in the MLCT drew both STS Linfa and TY Chan-Hom toward the northwest at the same time, its influence on drawing STS Linfa was stronger than TY Chan-Hom, because, unlike the deepening of Linfa's central pressure, TY Chan-Hom's central pressure with the maximum surface wind remained unchanged.

Similar to the movement of the MLCT (dark area in Figure 6a,b), TS Linfa moved from the east of Luzon Island in the Philippines toward the South China Sea. After it made landfall on Luzon Island in the morning of 5 July, it crossed over the northern part of the island in the afternoon and progressed further into the South China Sea on its west-northwest track. As TS Linfa entered the warm SST area of 31 °C, just to the southeast of Hong Kong, it gained moisture from thermal convection supplying water vapor from the warm sea surface via moisture flux into the lower atmosphere and also by transferring sufficient moisture into it from both the northeast-southwest oriented MLCT and northwestward moving TY Chan-Hom. In steering TS Linfa to the northwest, it re-intensified to a severe tropical storm like STS Linfa, deepening its central pressure by 5 hPa (Figures 7 and 8).

When latent heat is released by condensation of water vapor into water droplets (clouds) from the sea surface it increases the temperature in the air around the water droplets, which is the process known as thermal convection [27–30]. This process allows water vapor to ascend higher into the cloud and induces a cyclonic circulation which manifests itself in the atmosphere as convection in the center of a low-pressure system.

It means that the enhancement of vertical motion in the form of convection drives more latent heat through the condensation of water vapor into water droplets which are released in the upper troposphere, and effectively maintain the upper-level warm core, causing a typhoon to intensify. In turn, the released latent heating not only causes warm air

to rise but also enhances the instability of the troposphere, further enhancing convective activity from thermal convection [31–36].

(**a**) (**b**)
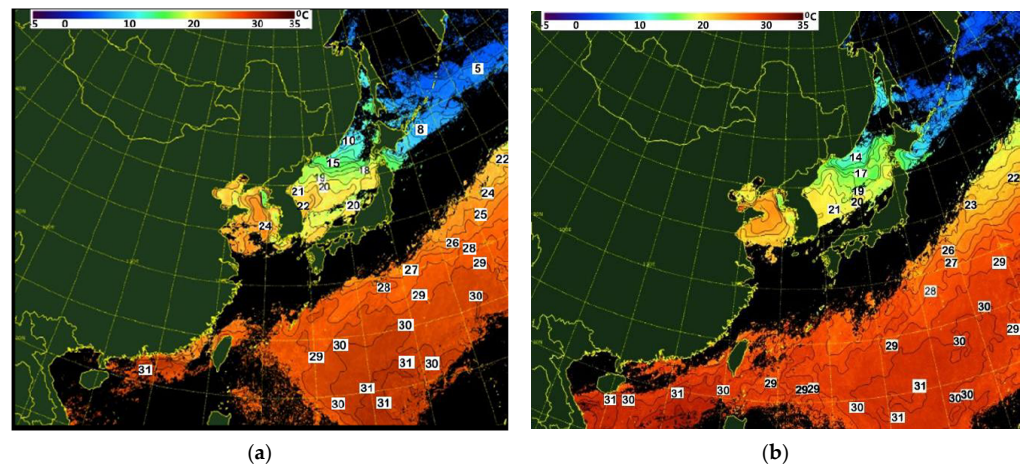
Figure 6. SST analysis (°C) at (**a**) 09:00 LST, 4 July 2015, and (**b**) 09:00 LST, 5 July. Long black areas oriented southwest to northeast in (**a**) and (**b**) indicate cloud bands, implying the MLCT corresponds to Figure 4a,b, and Figure 5a in (**a**) and Figures 7 and 8 in (**b**), respectively. STS Linfa moved to the South China Sea of 31 °C SST, passing by Luzon island of the Philippines. TY Chan-Hom also moved to the Kuroshio current of 31 °C SST in the east of the Philippines, gaining more energy from the warm sea to be intensified and the MLCT strongly attracts two typhoons in Figures 7 and 8.

(**a**) (**b**)
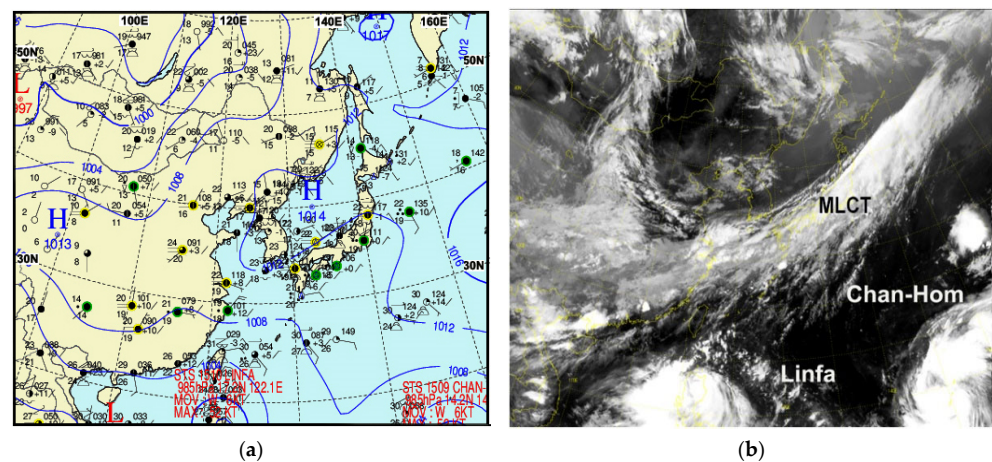
Figure 7. As shown in Figure 3, except for (**a**) surface pressure chart (hPa) and (**b**) COMS-IR satellite. image at 09:00 LST, 5 July.

The eastward movement in the MLCT steered the west-northwestward moving STS Linfa to a northerly direction causing an increase in maximum surface wind speed in the right quadrant of its cyclonic circulation, in addition to directly increasing moisture flux from thermal convection over the warm sea surface and indirectly from TY Chan-Hom, such that STS Linfa intensified and displayed an asymmetric distribution of wind speed. At 09:00 LST, 6 July, as the eastward movement in the MLCT pulled TY Chan-Hom to the northwest, the distance between them reduced. The subsequent interaction reinforced TY Chan-Hom's cyclonic circulation in its right upper quadrant, reducing its central pressure by 5 hPa to 980 hPa, a change in its maximum surface wind speed from 27 m/s1 to 29 m/s and an increase in speed to 19 km/h of the system itself.

(a)   (b)
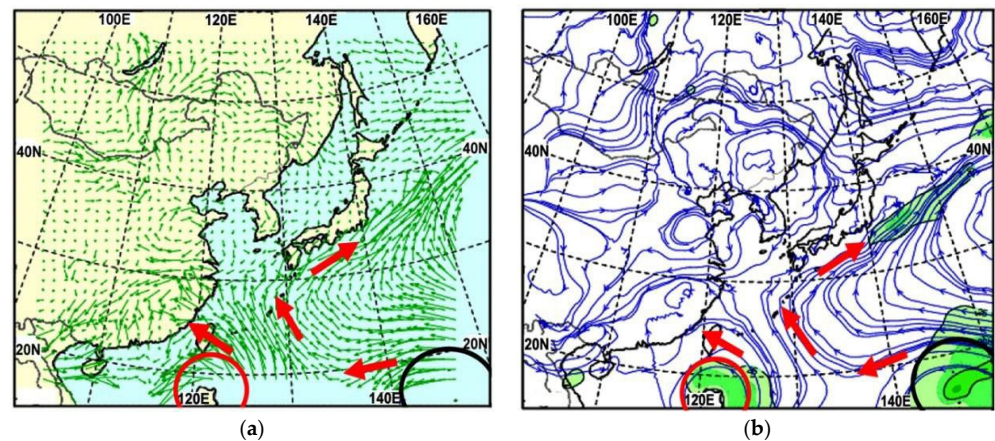
Figure 8. As shown in Figure 4, except for (**a**) moisture flux (0.1 kg·ms^{-1}) and (**b**) streamline with isotachs at 09:00 LST, 5 July. As the MLCT steered both STS Linfa and TY Chan-Hom northward, their cyclonic circulations in their upper quadrants enabled intensification from the strong southwest wind produced by the MLCT, and the decreasing distance between them then enhanced the exchange of moisture.

Owing to the influence of the MLCT, TY Chan-Hom moved northward into the area of 30 to 31 °C SST influenced by the Kuroshio warm current to the east of the Philippines and associated instability increased due to strong thermal convection of water vapor evaporated from the warm sea surface. Further intensification of its cyclonic circulation occurred due to the latent heat energy released from the condensation of water vapor to form clouds (Figures 9, 10, and 11a), similar to the re-intensification of STS Linfa on 5 July.

(a)   (b)
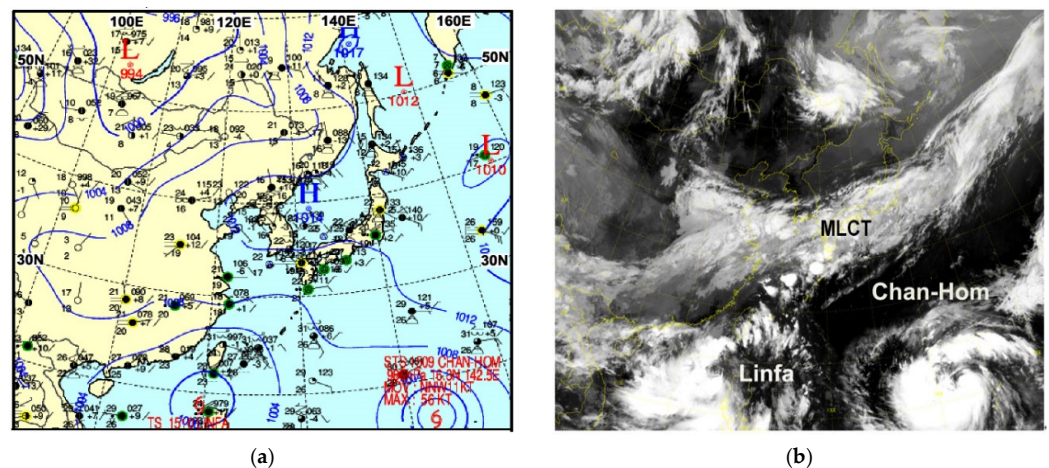
Figure 9. As shown in Figure 3, except for (**a**) surface pressure analysis (hPa) and (**b**) COMS-IR. satellite image at 09:00 LST, 6 July 2015. The multiple interactions between STS Linfa and TY Chan-Hom and between the MLTTC and TY Chan-Hom decreased the distance between them.

(**a**) (**b**)
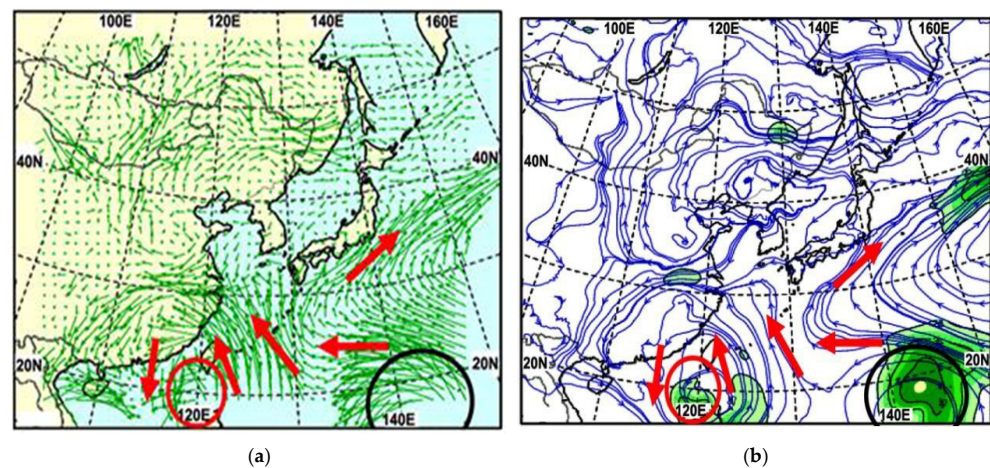
Figure 10. As shown in Figure 4, except for (**a**) moisture flux (0.1 kg·m/s) and (**b**) streamline with isotachs at 09:00 LST, 6 July. STS Linfa interacting with the MLCT was only weakly interacting with TY Chan-Hom until TY Chan-Hom transferred sufficient moisture into the circulation of Linfa as a result of the decreased distance between them. The moisture and momentum fluxes between STS Linfa and TY Chan-Hom, and also TY Chan-Hom and the MLCT were more intensified.

(**a**) (**b**)
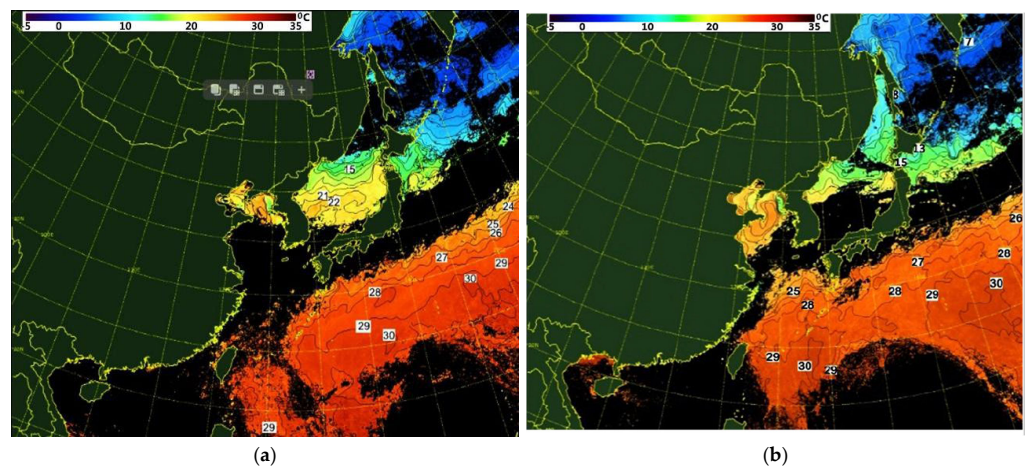
Figure 11. As shown in Figure 6, except recorded at (**a**) 09:00 LST, 6 July 2015, and (**b**) 09:00 LST, 7 July Long black areas indicate cloud bands in the MLCT. STS Linfa moved to the northern South China Sea of 31 °C SST near Macao passing by Luzon island. TY Chan-Hom moved over the Kuroshio current to the northeast of the Philippines of 31 °C SSTs, drawing STS Linfa and the MLCT.

In contrast to TY Chan-Hom, the central pressure of TS Linfa increased by 7 hPa to 992 hPa on 6 July, reducing its maximum surface wind from 27 ms^{-1} to 23 ms^{-1} due to the frictional effect of land including China, Taiwan Island, and the shallower sea bottom close to the coast (Table 1, Figure 9b). At the same time, as the westward movement of TY Chan-Hom was influenced by the MLCT, its resulting movement was more to the northwest, thereby decreasing the distance between STS Linfa and TY Chan-Hom.

This allowed TY Chan-Hom to disrupt Linfa's cyclonic circulation in its right upper quadrant and reduce surface wind speeds. Thus, as shown in Figure 10b, by the interaction of a stronger TY Chan-Hom connecting with the circulation of STS Linfa, Linfa was steered northwestward toward the Shantou area of Guangdong province in southern China.

By 09:00 LST, 7 July, TY Chan-Hom, having been steered northward by the MLCT over the area of 30~31 °C SST influenced by the Kuroshio current, had intensified by 5 hPa down to 975 hPa central pressure and maximum surface wind speed of 32 m/s in its the right-upper quadrant (Figures 11b, 12, and 13). On the other hand, STS Linfa moving

slowly at 4 km/h intensified by 7 hPa from a central pressure of 992 hPa to 985 hPa, and the maximum surface wind speed increased to 27 m/s.

(**a**)   (**b**)
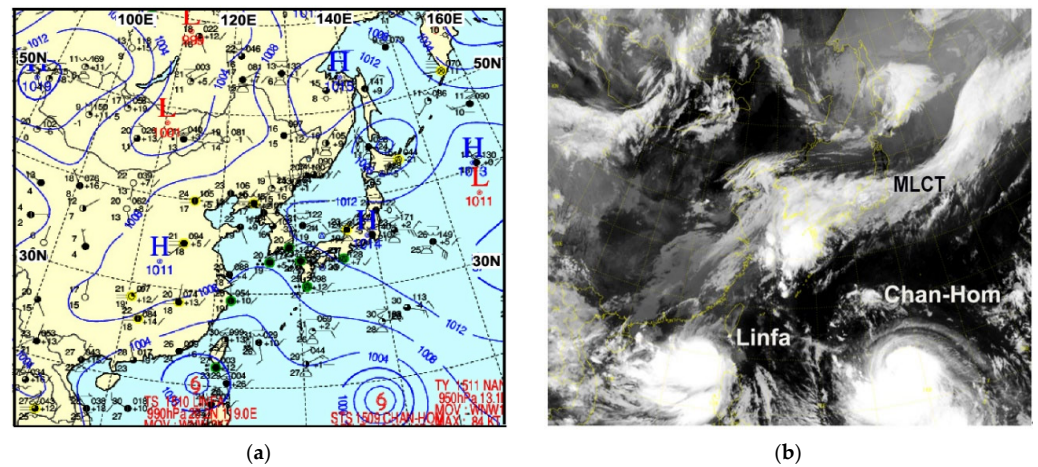
Figure 12. As shown in Figure 3, except for (**a**) surface pressure analysis (hPa), and (**b**) COMS-IR. satellite image at 09:00 LST 7 July. TS Linfa entering the northern part of the South China Sea increasingly interacted with TY Chan-Hom and the MLCT, as their distance decreased.

(**a**)   (**b**)
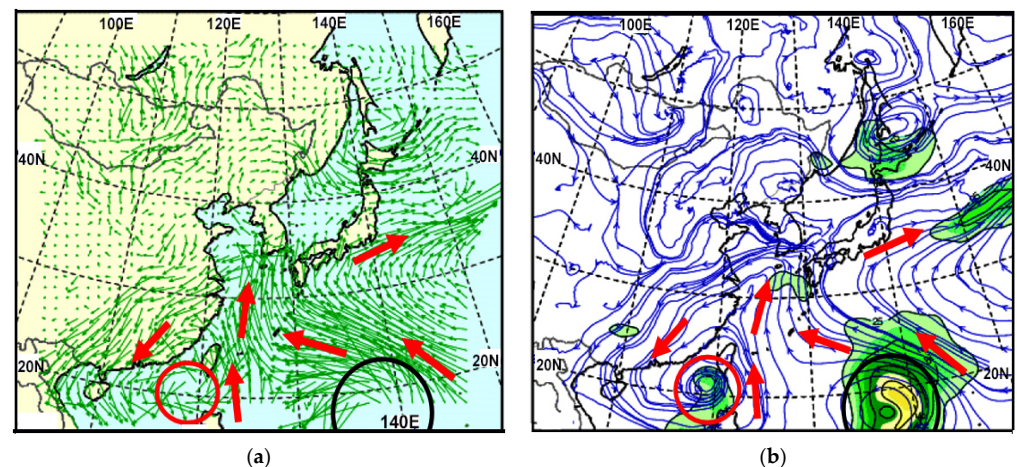
Figure 13. As shown in Figure 4, except for (**a**) moisture flux (0.1 m/s) and (**b**) streamline with isotaches at 09:00 LST, 7 July. STS Linfa develops by the intensified TY Chan-Hom pulled by the MLCT.

Even though STS Linfa was connected only weakly to the MLCT with a maximum wind speed of about 25 kt on the 850 hPa streamline analysis, it interacted with TY Chan-Hom by gaining in intensity and a greater wind speed in its right upper quadrant, due to the northward steering effect of the MLCT. This resulted in a decreasing distance between the two typhoons. For this reason, Linfa intensified by 7 hPa and a wind speed increase of 4 ms^{-1} and TY Chan-Hom intensified by 5 hPa with a wind speed increase of 3 m/s.

A new typhoon Nangka, which started as a tropical disturbance over the Marshall Islands on 1 July, was named the eleventh tropical storm on 4 July by the JTWC. At 09:00 LST, 7 July, it became a super typhoon with its central pressure having decreased rapidly to 950 hPa, a drop of 30 hPa from the previous day. This central pressure was much lower than those of the other two typhoons the previous day (Table 1). TY Nangka was moving quickly at 25 km/h with a maximum surface wind speed reaching 43 m/s.

COMS-IR satellite images at 09:00 LST, 8 July, showed that STS Linfa had turned to move west-northwest and then towards the eastern part of Guangdong province, China (Figures 14, 15, 16a, and 17a). TY Linfa and TY Chan-Hom were directly connected to each

other and the distance between the two tropical cyclones became even shorter due to the interaction of the strong northwest wind regime in the upper quadrant of their circulations resulting in a central pressure deepening of 15 hPa to 960 hPa for TY Chan-Hom and a maximum surface wind speed of 39 m/s.

(a)   (b)
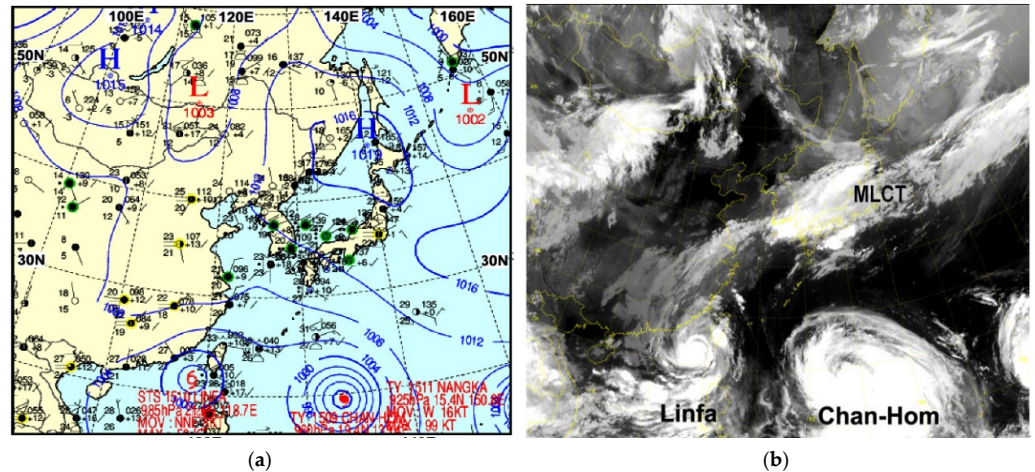
Figure 14. As shown in Figure 3, except for (**a**) surface pressure analysis (hPa), and (**b**) COMS-IR. satellite image at 09:00 LST, 8 July. STS Linfa remained stationary owing to TY Chan-Hom intensifying from interaction with TY Nangka behind but its distance to TY Chan-Hom decreased.

(a)   (b)
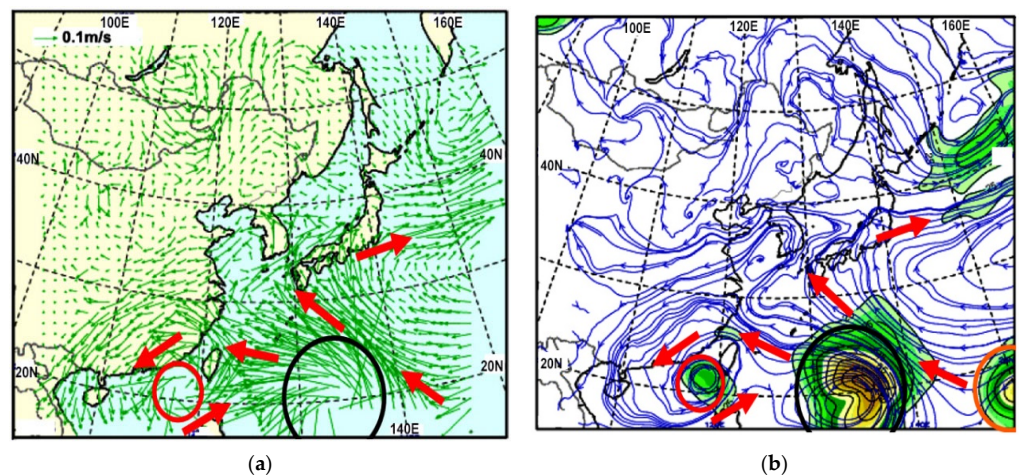
Figure 15. As shown in Figure 4, except for (**a**) moisture flux (0.1 kg·m/s) and (**b**) streamline with isotaches at 09:00 LST, 8 July. In (**b**), as STS Linfa (left) was strongly pulled by the more intensified TY Chan-Hom (center) by mutual interaction of the MLCT and TY Nangka (right), it kept the same central pressure and maximum wind speed.

At this time, with TY Chan-Hom still strongly interacting with the MLTTC and connected to TY Nangka, which had deepened 25 hPa in 24 h to 925 hPa and following in the path of TY Chan-Hom, the distance between TY Chan-Hom and TY Nangka rapidly decreased. By interacting with TY Chan-Hom the cyclonic circulation of TY Linfa was disrupted, and its westward movement was hindered.

As a result, Linfa maintained almost the same position as the previous day, in addition to the same central pressure value and maximum surface wind speed. The complex interactions shown with the three tropical cyclones produced asymmetric wind distribution in their cyclonic circulations, particularly highlighting the greater surface wind speeds in the upper right quadrants of their circulations.

(a)　　　　　　　　　　　　　　　　(b)
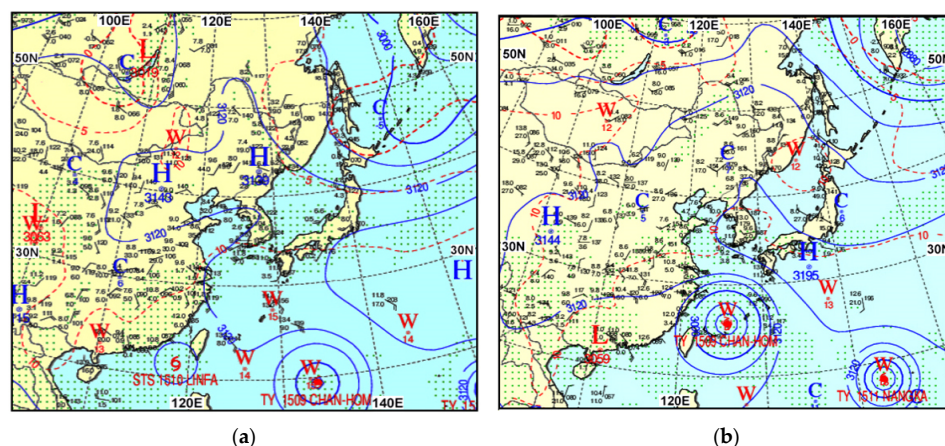
Figure 16. (**a**) Geopotential analysis (m) at 700 hPa (3 km height) at 09:00 LST, 8 July, and (**b**) at 09:00 LST, 10 July. Small green-colored dots from southwest to northeast denote the MLCT. In (**b**), STS Linfa making landfall on the Chinese coast weakened to low pressure by increasing friction of the land and shallower sea bed. The much stronger TY Chan-Hom absorbed moisture from STS Linfa and weakened its circulation, causing the dissipation of Linfa finally.

(a)　　　　　　　　　　　　　　　　(b)
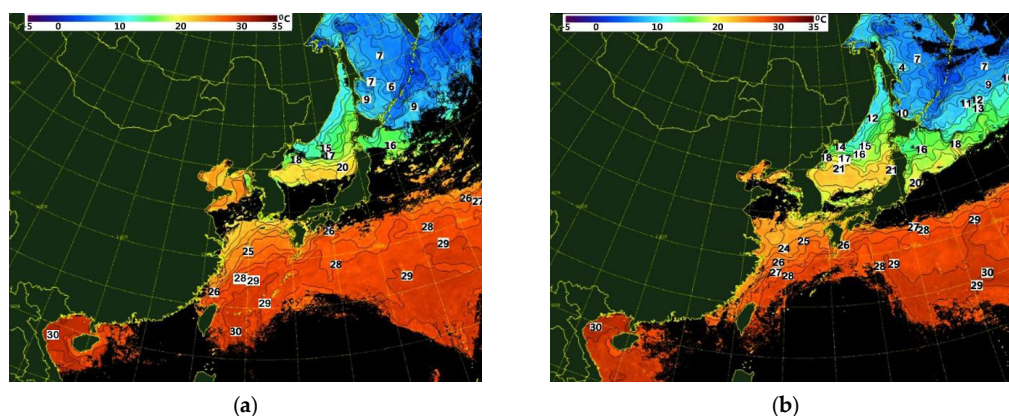
Figure 17. (**a**) Images taken at 09:00 LST, 8 July 2015, and (**b**) 09:00 LST, 9 July. Long black area oriented from southwest to northeast in (**a**,**b**) indicates the MLCT. STS Linfa moved to the warmest sea of 31 °C SST in the South China Sea passing Luzon Island in (**a**,**b**). TY Chan-Hom also moved over the Kuroshio current of 31 °C SST to the northeast of the Philippines, being closer to the MLCT.

At 06:00 UTC, 9 July, Linfa had further intensified with central pressure down to 980 hPa as it moved westward at 13 km/h toward Macao with a maximum surface wind speed of 29 m/s. At 09:00 LST, TY Chan-Hom had intensified to a central pressure of 955 hPa and a maximum wind speed of 40 m/s, owing to its now close proximity to TY Nangka and hence strong interaction by the northwest steering from TY Nangka and northeast steering from the MLCT.

As a result, TY Nangka rapidly further intensified down to 935 hPa central pressure and 49 m/s maximum surface wind speed (Figures 17b and 18). Thus, even though STS Linfa made landfall at Lufeng City, Guangdong province, and continued to move westward. Instead of weakening, it strengthened by mutual feedback of moisture and momentum fluxes with the recently intensified TY Chan-Hom, producing a maximum surface wind speed of 29 m/s (Figure 19a,b).
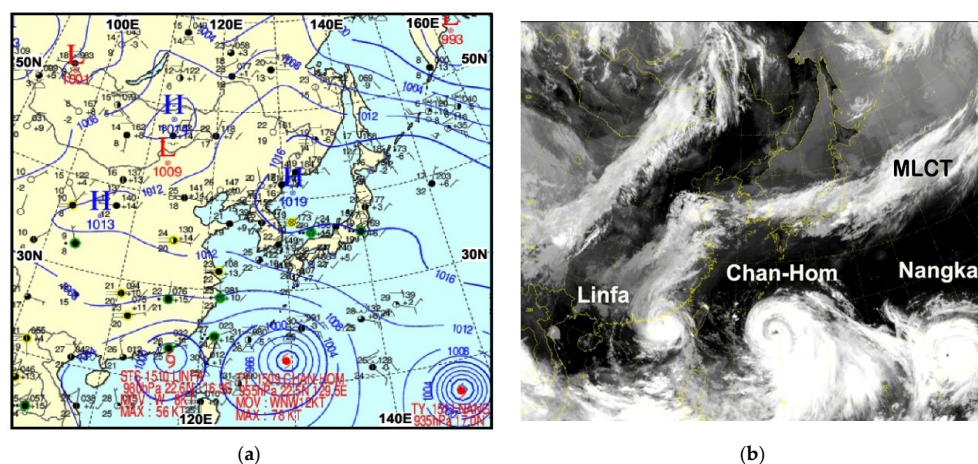
Figure 18. As shown in Figure 3, except for (**a**) surface pressure analysis (hPa) and (**b**) COMS-IR satellite image, at 09:00 LST, 9 July. In (**b**), MLCT indicated (center right), Typhoon Linfa just before landfall, and TY Chan-Hom cloud interaction with TY Nangka.
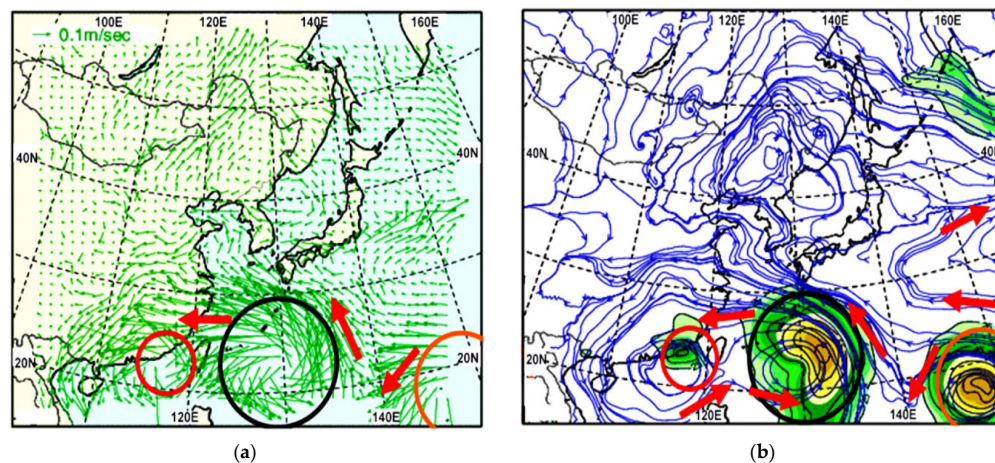
Figure 19. As shown in Figure 4, except for (**a**) moisture flux (0.1 kg·m/s) and (**b**) streamline with isotaches at 09:00 LST, 9 July 2015. STS Linfa, TY Chan-Home, and TY Nangka became closer to each other as a result of multiple interactions among them.

From the numerical simulation using WRF-3.6 meteorological model, Figure 20a,b shows the distributions of relative humidity and wind speed at 1.5 km height (about 850 hPa level), similar to Figure 21a,b at 5 km height (about 500 hPa level). The mutual feedback of moisture and momentum fluxes among the three typhoons and the MLCT is much stronger at 5 km height than at 1.5 km height but cloud bands along the MLCT above 5 km height are weak rather than at 1.5 km height because the moisture in the air to be sparse. Since TY Nangka, TY Chan-Hom, and TY Lifa are strongly connected in a gale belt with the MLCT at 5 km height, it is apparent that the convergence of the air is along the MLCT. Thus, the mutual interactions of the MLCT with three typhoons are very important to the intensification and decay of each typhoon.
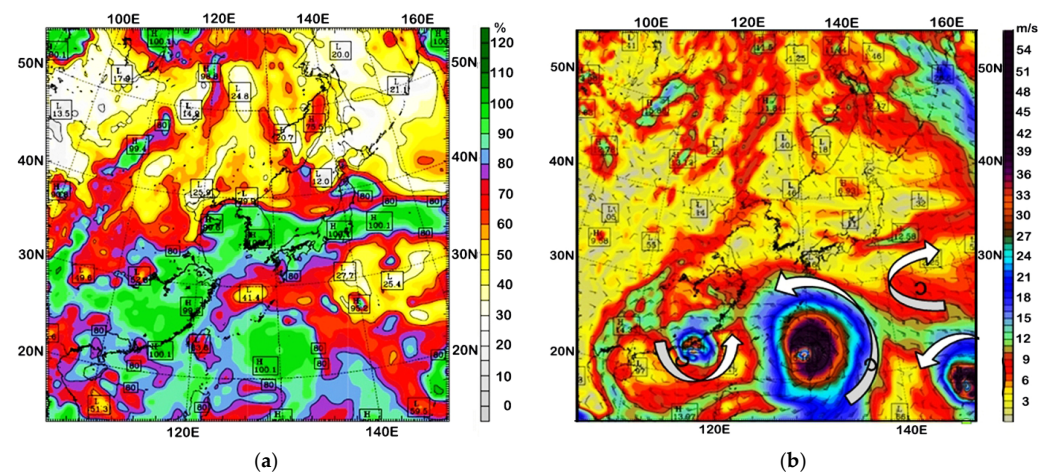
Figure 20. (**a**) Relative humidity (%) and (**b**) wind (m/s) at 1.5 km height (850 hPa) by WRF-3.6 model at 09:00 LST, 9 July 2015. The three typhoons' steering as a result of multiple interactions among them (STS Linfa (bottom-left), TY Chan-Home (bottom-center), and TY Nangka (bottom-right)) cause their intensification and decay.
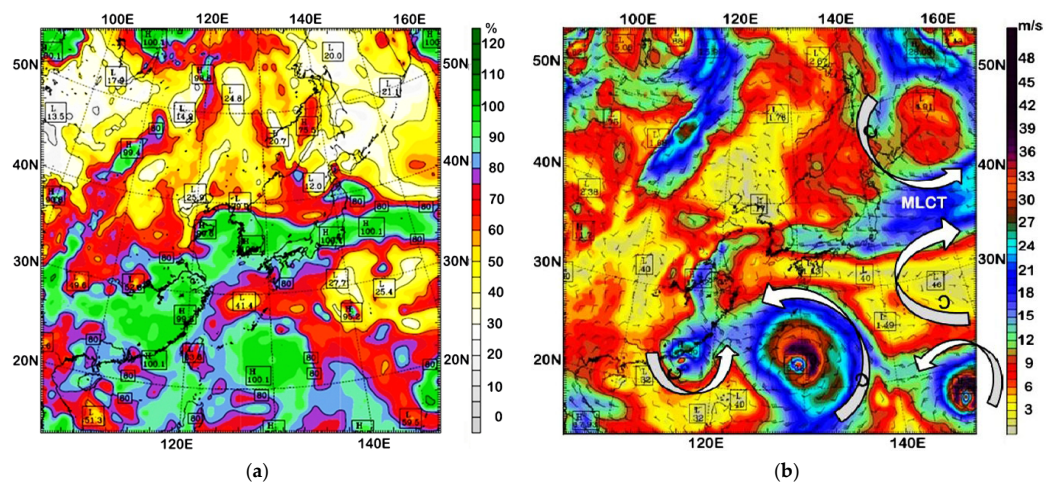
Figure 21. As shown in Figure 20, except for relative humidity (**a**) and (**b**) wind speed (m/s) 5 km height. The three typhoons became much closer to each other with stronger multiple interactions. Though STS Linfa made landfall at Lufeng city and moved westward instead of weakening, it strengthened by mutual feedback of moisture and momentum fluxes with the more intensified TY Chan-Hom better than at 1.5 km height.

On 10 July, TY Chan-Hom continued to develop as it passed between the Japanese islands of Okinawa and Miyako-Jima with a central pressure of 935 hPa and peak wind strength of 49 m/s. As STS Linfa passed Macao on its northward track, it weakened rapidly to a tropical depression and later to a low-pressure system with a central pressure of 1000 hPa due to the increasing friction over land in the Guangdong province and the shallower sea bottom. Thus, the much more intense TY Chan-Hom absorbed moisture from closely interacting with STS Linfa whose circulation was maintained after its landfall in Macao (Figures 22 and 23).

(**a**)   (**b**)
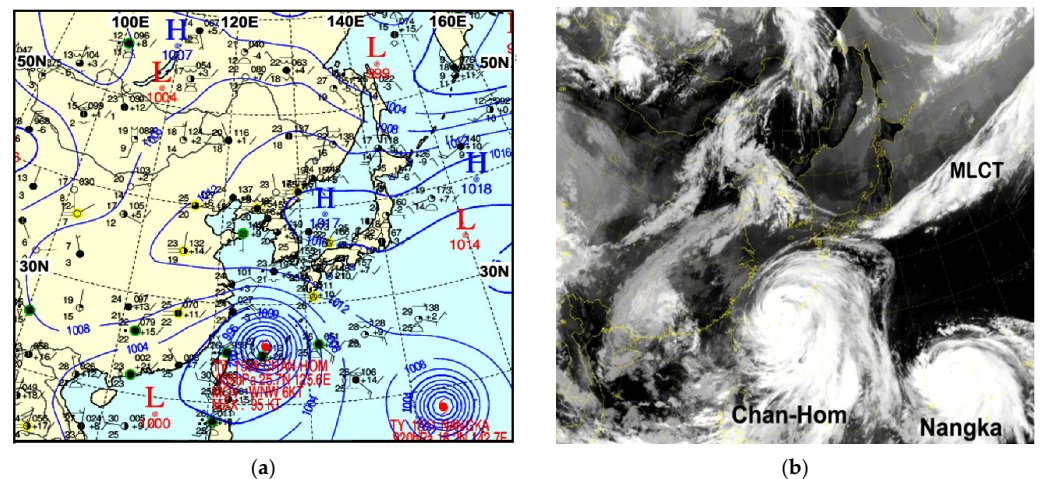
Figure 22. As shown in Figure 3, except for (**a**) surface pressure chart (hPa) and (**b**) COMS-IR satellite image, at 09:00 LST, 10 July 2015. STS Linfa's circulation weakened to a low pressure (L; 1000 hPa, finally dissipating, because of its strong interaction with TY Chan-Hom and the friction of the inland and shallower sea depth.

(**a**)   (**b**)
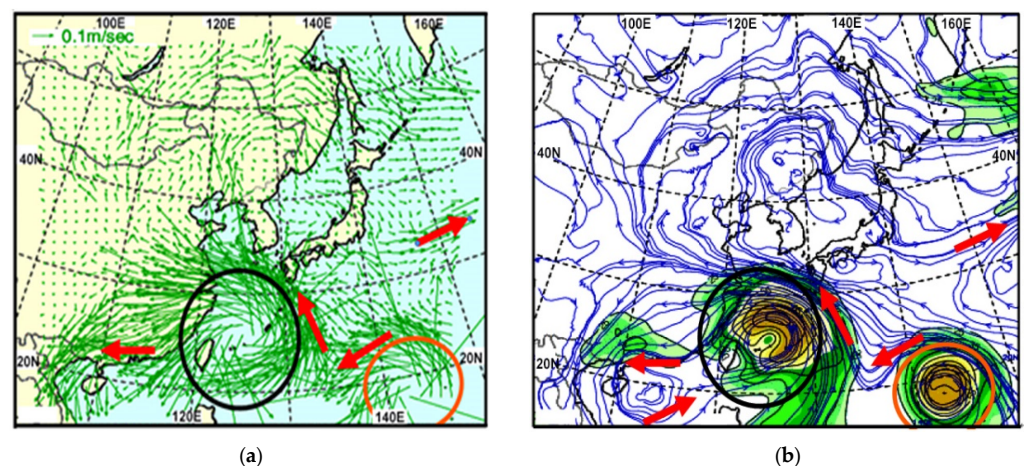
Figure 23. As shown in Figure 4, except for (**a**) moisture flux (0.1·kg.m/s) and (**b**) streamline with isotaches (green-color areas greater than 25 kt) at 850 hPa (1.5 km height) at 09:00 LST, 10 July 2015. TY Chan-Hom interacted with TY Nangka and an MLCT resulting in northward movement. As STS Linfa made landfall, it weakened to a low pressure to finally dissipate, because of friction of the land and shallower sea bottom.

TY Chan-Hom still maintained the same central pressure of 935 hPa but owing to its interaction with STS Linfa its maximum surface wind speed increased to 49 m/s. Similarly, TY Nangka also intensified down to 920 hPa central pressure and a maximum surface wind speed of 53 m/s. Therefore, both TY Chan-Hom and TY Nangka were re-enforced as the distance between them decreased from the strong interaction and broadened to a tail-shaped area of increase in wind speed in the right quadrant circulation of TY Chan-Hom.

4. Conclusions

In July 2015, six typhoons were active in the western Pacific Ocean. Forecasting their tracks from day to day by Asian National Weather Organizations was made difficult owing to complex interactions between them and other meteorological phenomena. This study focused on the development and decay of STS Linfa through its multiple interactions with two typhoons TY Chan-Hom and TY Nangka, and a mid-latitude cloud band-associated trough (MLCT).

As STS Linfa entered SSTs, reaching 31 °C southeast of Hong Kong, the system gained a lot of moisture from strong thermal convection supplying water vapor to the lower atmosphere, which condensed to form clouds and released latent heat in the process. In addition, moisture was transferred to the system from the interaction caused by the northeast movement in an MLCT and the northwest movement of TY Chan-Hom. In changing direction toward the northwest, STS Linfa was also re-intensified to a severe tropical storm with large cloud clusters and a lower (more intense) central pressure.

Focusing on STS Linfa and its interaction with the other systems the processes involved can be summarized according to the following sequence:

(1) The southwesterly wind ahead of the MLCT steered both STS Linfa and TY Chan-Hom west-northwest after both initially were steered independently to the northwest. Linfa's cyclonic circulation intensified in its right upper quadrant turning it into a severe tropical storm without any change to Chan-Hom. As STS Linfa entered the area of 31 °C SST in the northern part of the South China Sea, it gained much more moisture due to both strong thermal convections containing water vapor from the warm sea surface and receiving a large amount of moisture from the MLCT due to their interaction, which caused Linfa to further develop;

(2) As STS Linfa approached the coast, the friction of the shallower sea bottom and of the mainland of southern China itself weakened its circulation. However, the circulation of TY Chan-Hom over the open sea intensified while its interaction with the northeastward movement of the MLCT inhibited Linfa's cyclonic circulation and weakened it the closer it became to the MLCT;

(3) Eventually, STS Linfa became disconnected from the MLCT and re-intensified by interacting with the more powerful TY Chan-Hom, which was moving toward the warm SST area of 30~31 °C associated with the Kuroshio Current. Enhanced moisture flux from TY Chan-Hom interacted with the strongly intensified TY Nangka and the moisture flux transferred into STS Linfa causing further development from the latent heat of condensation to form cloud clusters;

(4) Finally, as STS Linfa made landfall on the coast of southern China, increased friction from both the shallow sea bottom adjacent to the coast and the land itself, in addition to moisture transfer from STS Linfa to the more intense TY Chan-Hom, resulted in STS Linfa weakening into a weak low-pressure system before dissipating.

References

1. Anthes, R.A.; Chang, S.W. Response of the Hurricane Boundary Layer to Changes of Sea Surface Temperature in a Numerical Model. *J. Atmos. Sci.* **1978**, *135*, 1240–1255. [CrossRef]
2. Choi, H. Extreme decrease of air temperature modified by a typhoon passage in the Korean eastern coast. *Disaster Adv.* **2012**, *5*, 45–51.
3. Hong Kong Meteorological Observatory (HKO). In *Classification of Tropical Cyclones*; 2012. Available online: http://www.hko.gov. hk/informtc/class.html (accessed on 10 September 2012).
4. World Meteorological Organization (WMO). Guidelines for Converting between Various Wind Averaging Periods in Tropical Cyclone Conditions. 2010, pp. 1–63. Available online: https://library.wmo.int/index.php?lvl=notice_display&id=135#.ZDPa3 3ZByUk (accessed on 10 September 2012).
5. Korea Meteorological Administration (KMA). 2013. Available online: http://www.kma.go.kr/ (accessed on 10 September 2012).
6. Choi, H. Extreme cold sea outbreak near Cheju Island, Korea by strong wind and atmospheric pressure change under typhoon Rusa. *Disaster Adv.* **2010**, *3*, 32–41.
7. Choi, H.; Lee, M.S.; Choi, S.M. Cold sea surface temperature near Cheju Island responding to strong cyclone wind and positive geopotential tendency behind a typhoon center along its track. *J. Mar. Sci. Technol.* **2012**, *20*, 684–692. [CrossRef]
8. Subrahmanyam, M.V. Impact of typhoon on the north-west Pacific sea surface temperature: A case study of Typhoon Kaemi. *Nat. Hazards* **2006**, *78*, 569–582. [CrossRef]
9. Latif, M.; Keenlyside, N.; Bader, J. Tropical sea surface temperature, vertical wind shear, and hurricane development. *Geophys. Res. Lett.* **2007**, *34*, 1–4. [CrossRef]
10. Feng, G.; Subrahmanyam, M.V. Chlorophyll variations over coastal area of China due to typhoon Rananim. *Indian J. Mar. Sci.* **2018**, *47*, 804–811.
11. Price, J.F. Upper ocean response to a hurricane. *J. Phys. Ocean.* **1981**, *11*, 153–175. [CrossRef]
12. Gill, A.E. *Atmosphere-Ocean Dynamics*; Academic Press: New York, NY, USA, 1982; pp. 1–662.
13. Knauss, J.A. *Introduction to Physical Oceanography*, 2nd ed.; Waveland Press, Inc.: Long Grove, IL, USA, 1997; pp. 1–309.
14. Franklin, J.L.; Lord, S.J.; Feuer, S.E.; Marks, F.D., Jr. The Kinematic Structure of Hurricane Gloria (1985) Determined from Nested Analyses of Dropwindsonde and Doppler Radar Data. *Mon. Weather. Rev.* **1993**, *121*, 2433–2451. [CrossRef]
15. Sheng, J.; Zhai, X.; Greatbatch, R.J. Numerical study of the storm-induced circulation on the Scotian Shelf during Hurricane Juan using a nested-grid ocean model. *Prog. Oceanogr.* **2006**, *70*, 233–254. [CrossRef]
16. Cheung, T.C.; Chan, P.W. Improving Wind and Rain Simulations for Tropical Cyclones with the Assimilation of Doppler Radar Data. In Proceedings of the 10th Annual WRF Users' Workshop, Boulder, CO, USA, 23–26 June 2009; pp. 1–835.
17. Dhana, L.D.; Annapurnaiah, K. Impact of microphysical schemes in the simulations of cyclone Hudhud using WRF-ARW model to find out the best microphysics for accurate simulation of intensity and track of tropical cyclone. *Int. J. Oceans Ocean.* **2016**, *10*, 49–59.
18. Shyam, A.; Sharma, N. Ocean surface winds from Aquarius L-band Radiometer during Tropical Cyclones: Case Studies. *Int. J. Oceans Ocean.* **2018**, *12*, 147–158.
19. Fujiwhara, S. The natural tendency towards symmetry of motion and its application as a principle in meteorology. *Q. J. R. Meteorol. Soc.* **1921**, *47*, 287–292. [CrossRef]
20. Liu, K.Y. *On the Relative Motion of Typhoon Pairs Over the South China Sea and Northwest Pacific Region*; NSC73-0202-M072-02; NSC: Taipei, China, 1983; pp. 1–38.
21. DeMaria, M.; Chan, J.C.L. Comments on "A Numerical Study of the Interactions between Two Tropical Cyclones". *Mon. Weather. Rev.* **1983**, *112*, 1643–1645. [CrossRef]
22. Kuo, H.-C.; Chen, G.T.-J.; Lin, C.-H. Merger of Tropical Cyclones Zeb and Alex. *Mon. Weather. Rev.* **2000**, *128*, 2967–2975. [CrossRef]
23. Xu, H.; Zhang, X.; Xu, X. Impact of Tropical Storm Bopha on the Intensity Change of Super Typhoon Saomai in the 2006 Typhoon Season. *Adv. Meteorol.* **2013**, *2013*, 487010. [CrossRef]
24. Choi, H.; Lee, M.S. Tropical storm Sarika merging in Typhoon Songda circulation by strong wind and sufficient moisture transportation. *Disaster Adv.* **2015**, *8*, 1–7.
25. Yeh, K.D.; Liu, J.C.; Eea, M.; Lin, C.H.; Lu, W.L.; Chiang, C.T.; Lee, Y.S.; Chen, A.H.C. Intensification and decay of typhoon Nuri (2014) associated with cold front and southwesterly airflow observed in satellite cloud images. *J. Mar. Sci. Technol.* **2017**, *25*, 599–606. [CrossRef]
26. Wikipedia. North Pacific High. 2023. Available online: https://en.wikipedia.org/wiki/North_Pacific_High (accessed on 10 September 2012).
27. Wikipedia. 2015 Pacific Typhoon Season. 2015. Available online: https://en.wikipedia.org/wiki/2015_Pacific_typhoon_season (accessed on 10 September 2012).
28. Danard, M.B. On the Influence of Released Latent Heat on Cyclone Development. *J. Appl. Meteorol.* **1964**, *3*, 27–37. [CrossRef]
29. Miller, W.; Chen, H.; Zhang, D.L. On the intensification of Hurricane Wilma (2005), Part III: Effects of latent heat of fusion. *J. Atmos. Sci.* **2015**, *72*, 3829–3849. [CrossRef]
30. Li, M.; Ping, F.; Chen, J.; Xu, L. A simulation study on the rapid intensification of Typhoon Megi (2010) in vertical wind shear. *Atmospheric Sci. Lett.* **2016**, *17*, 630–638. [CrossRef]

31. DeMaria, M.; Kaplan, J. Sea Surface Temperature and the Maximum Intensity of Atlantic Tropical Cyclones. *J. Clim.* **1994**, *7*, 1324–1334. [CrossRef]
32. DeMaria, M. The effect of vertical shear on tropical cyclone intensity change. *J. Atmos. Sci.* **1996**, *53*, 2076–2087. [CrossRef]
33. Frank, W.M.; Ritchie, E.A. Effects of Vertical Wind Shear on the Intensity and Structure of Numerically Simulated Hurricanes. *Mon. Weather. Rev.* **2001**, *129*, 2249–2269. [CrossRef]
34. Corbosiero, K.L.; Molinari, J. The Effects of Vertical Wind Shear on the Distribution of Convection in Tropical Cyclones. *Mon. Weather. Rev.* **2000**, *130*, 2110–2123. [CrossRef]
35. Riemer, M.; Montgomery, M.T.; Nicholls, M.E. Further examination of the thermodynamic modification of the inflow layer of tropical cyclones by vertical wind shear. *Atmos. Chem. Phys. Discuss.* **2013**, *13*, 327–346. [CrossRef]
36. Chen, H.; Zhang, D.-L. On the Rapid Intensification of Hurricane Wilma (2005). Part II: Convective Bursts and the Upper-Level Warm Core. *J. Atmos. Sci.* **2013**, *70*, 146–162. [CrossRef]